JOURNAL OF APPLIED CRYSTALLOGRAPHY

Volume 50 (2017)

Supporting information for article:

Modeling the polarized X-ray scattering from periodic nanostructures with molecular anisotropy

Christopher D. Liman, Thomas A. Germer, Daniel F. Sunday, Dean M. DeLongchamp and R. Joseph Kline

Modeling the polarized X-ray scattering from periodic nanostructures with molecular anisotropy

Christopher D. Liman[a], Thomas A. Germer[b], Daniel F. Sunday[a], Dean M. DeLongchamp[a], R. Joseph Kline[a]*

[a]Materials Science and Engineering Division, National Institute of Standards and Technology, 100 Bureau Drive, Gaithersburg, MD 20899, USA

[b]Sensor Science Division, National Institute of Standards and Technology, 100 Bureau Drive, Gaithersburg, MD 20899, USA

*joe.kline@nist.gov

Supporting Information

Born approximation simulation

Solutions to Fourier transforms

The form factor for a trapezoid with constant scattering length density ρ_T (equations 4-6 in the main text) is:

$$\rho_T \int_{z_1}^{z_2} \int_{x_a(z)}^{x_b(z)} e^{-iq_x x} e^{-iq_z z}\, dx\, dz$$

$$= \rho_T \frac{z_1 - z_2}{q_x} e^{-iq_z(z_1+z_2)} \left(\frac{e^{i(q_z z_1 - q_x x_2)} - e^{i(q_z z_2 - q_x x_1)}}{q_x(x_1 - x_2) + q_z(z_1 - z_2)} + \frac{e^{i(q_z z_1 - q_x x_3)} - e^{i(q_z z_2 - q_x x_4)}}{q_x(x_3 - x_4) + q_z(z_2 - z_1)} \right). \quad \text{(SI1)}$$

The interface component of the form factor for a trapezoid with orientation strength varying with horizontal distance from the interface (equations 14-16 in the main text) is:

$$\int_{z_1}^{z_2} \int_{x_a(z)}^{x_b(z)} \left(e^{-x_l(x,z)/l_p} + e^{-x_r(x,z)/l_p} \right) e^{-iq_x x} e^{-iq_z z}\, dx\, dz$$

$$= l_p(z_1 - z_2) \left(\frac{e^{-i(q_x x_4 + q_z z_1) + (x_1 - x_4)/l_p} - e^{-i(q_x x_3 + q_z z_2) + (x_2 - x_3)/l_p}}{(l_p q_x - i)(q_x(x_4 - x_3) + q_z(z_1 - z_2) + i(x_1 - x_2 + x_3 - x_4)/l_p)} \right.$$

$$- \frac{e^{-i(q_x x_1 + q_z z_1) + (x_1 - x_4)/l_p} - e^{-i(q_x x_2 + q_z z_2) + (x_2 - x_3)/l_p}}{(l_p q_x + i)(q_x(x_1 - x_2) + q_z(z_1 - z_2) + i(x_1 - x_2 + x_3 - x_4)/l_p)}$$

$$- \frac{e^{-i(q_x x_1 + q_z z_1)} - e^{-i(q_x x_2 + q_z z_2)}}{(l_p q_x - i)(q_x(x_1 - x_2) + q_z(z_1 - z_2))}$$

$$\left. - \frac{e^{-i(q_x x_4 + q_z z_1)} - e^{-i(q_x x_3 + q_z z_2)}}{(l_p q_x + i)(q_x(x_4 - x_3) + q_z(z_1 - z_2))} \right). \quad \text{(SI2)}$$

Derivation of scattering contrast

We derive an expression for the scattering length density of each trapezoid, ρ_T, that takes into account the molecular orientation-dependent interaction between the resonant X-rays and the transition dipole

moments of the antibonding orbitals. We start with the normalized electric field of the incident X-rays, $\hat{E}_{\mathrm{in}}$, which induces a dipole moment

$$\vec{p} = \boldsymbol{\alpha} \cdot \hat{E}_{\mathrm{in}}, \tag{SI3}$$

where $\boldsymbol{\alpha}$ is the second-rank complex polarizability tensor. This dipole moment then radiates an electric field $\vec{E}_{\mathrm{scat}}$ in the radiation zone (Jackson, 1999) (eqn. 9.19),

$$\vec{E}_{\mathrm{scat}} = \left(\frac{\mu_0}{\epsilon_0}\right)^{1/2} \frac{ck^2}{4\pi} \frac{e^{ikr}}{r} \left((\hat{n} \times \vec{p}) \times \hat{n}\right), \tag{SI4}$$

where $\hat{n}$ is a unit vector in the direction of the scattered Poynting vector, k is the wave number, r is the distance between the scatterer and the observer, c is the speed of light, μ_0 is the vacuum permeability and ϵ_0 is the vacuum permittivity.

Using the identity $\left(\vec{a} \times \vec{b}\right) \times \vec{c} = (\vec{c} \cdot \vec{a})\vec{b} - \left(\vec{c} \cdot \vec{b}\right)\vec{a}$, equation (SI4) can be rewritten as:

$$\vec{E}_{\mathrm{scat}} = \left(\frac{\mu_0}{\epsilon_0}\right)^{1/2} \frac{ck^2}{4\pi} \frac{e^{ikr}}{r} [\vec{p} - (\hat{n} \cdot \vec{p})\hat{n}]. \tag{SI5}$$

We express $\vec{p}$ in terms of the direction of propagation $\hat{n}$, a unit vector in the direction of $\vec{E}_{\mathrm{scat}}$, $\hat{E}_{\mathrm{scat}}$, and an additional orthogonal basis vector $\hat{m} = \hat{n} \times \hat{E}_{\mathrm{scat}}$:

$$\vec{p} = (\hat{n} \cdot \vec{p})\hat{n} + \left(\hat{E}_{\mathrm{scat}} \cdot \vec{p}\right)\hat{E}_{\mathrm{scat}} + (\hat{m} \cdot \vec{p})\hat{m}. \tag{SI6}$$

Thus, we have

$$\vec{E}_{\mathrm{scat}} = \left(\frac{\mu_0}{\epsilon_0}\right)^{1/2} \frac{ck^2}{4\pi} \frac{e^{ikr}}{r} \left[\left(\hat{E}_{\mathrm{scat}} \cdot \vec{p}\right)\hat{E}_{\mathrm{scat}} + (\hat{m} \cdot \vec{p})\hat{m}\right]. \tag{SI7}$$

Placing equation (SI3) into the above:

$$\vec{E}_{\mathrm{scat}} = \left(\frac{\mu_0}{\epsilon_0}\right)^{1/2} \frac{ck^2}{4\pi} \frac{e^{ikr}}{r} \left[\left(\hat{E}_{\mathrm{scat}} \cdot \boldsymbol{\alpha} \cdot \hat{E}_{\mathrm{in}}\right)\hat{E}_{\mathrm{scat}} + \left(\hat{m} \cdot \boldsymbol{\alpha} \cdot \hat{E}_{\mathrm{in}}\right)\hat{m}\right] \tag{SI8}$$

Since $\hat{E}_{\mathrm{scat}}$ was defined to be in the direction of $\vec{E}_{\mathrm{scat}}$, we can drop the second term in the expression above and derive our final expression for the scattering length density ρ_T:

$$\rho_T \propto \hat{E}_{\mathrm{scat}} \cdot \boldsymbol{\alpha} \cdot \hat{E}_{\mathrm{in}} \tag{SI9}$$

Derivation of diffraction efficiency

We assume that the incident electric field is given by

$$\vec{E}_{\mathrm{in}}(\vec{r}) = \vec{E}_{\mathrm{in}} \exp\left(ik_{0,z}z\right) \exp\left(ik_{0,x}x\right), \tag{SI10}$$

where $k_{0,x} = k \sin\theta_0$, $k_{0,z} = k \cos\theta_0$, $k = 2\pi/\lambda$, and θ_0 is the incident angle. The power per unit area associated with this wave is

$$P^{(0)} = \frac{\cos\theta_0}{2} Z_0 \left|\vec{E}_{\mathrm{in}}\right|^2, \tag{SI11}$$

where Z_0 is the impedance of free space. At the location of the grating, the field is attenuated due to absorption in the substrate and is reduced to

$$\vec{E}^{(0)}(\vec{r}) = \vec{E}_{\text{in}} \exp\left(ik_{0,z}z\right) \exp\left(ik_{0,x}x\right) \exp\left(-\frac{\mu\tau}{2\cos\theta_0}\right), \tag{SI12}$$

where $\mu = (4\pi/\lambda)\ \text{Im}\ n_s$, and τ is the thickness of the substrate. The scattered (diffracted) field above the structure is a Floquet series in x,

$$\vec{E}(\vec{r}) = \sum_j \vec{E}_j \exp\left(ik_{j,z}z\right) \exp(ik_{j,x}x)\,, \tag{SI13}$$

where d is the period, $k_{j,x} = jQ + k_{0,x} = k\sin\theta_j$, $k_{j,z} = \left(k^2 - k_{j,x}^2\right)^{1/2} = k\cos\theta_j$, and

$$\vec{E}_j = \frac{1}{d}\int_0^d \vec{E}(\vec{r}) \exp\left(-ik_{j,x}x\right) dx\,. \tag{SI14}$$

The power per unit area associated with $\vec{E}_j$ is

$$P_j = \frac{\cos\theta_j}{2} Z_0 \left|\vec{E}_j\right|^2, \tag{SI15}$$

Thus, the diffraction efficiency is

$$\frac{P_j}{P^{(0)}} = \frac{\cos\theta_j}{\cos\theta_0} \frac{\left|\vec{E}_j\right|^2}{\left|\vec{E}_{\text{in}}\right|^2}. \tag{SI16}$$

In the Born approximation, we solve the wave equation

$$\nabla \times \left(\nabla \times \vec{E}(\vec{r})\right) - k^2 \vec{E}(\vec{r}) = -k^2 \Delta\overleftrightarrow{\epsilon}(\vec{r}) \vec{E}^{(0)}(\vec{r}), \tag{SI17}$$

where by $\Delta\overleftrightarrow{\epsilon}(\vec{r}) = \overleftrightarrow{\epsilon}(\vec{r}) - 1$ is the modulation in the dielectric tensor $\overleftrightarrow{\epsilon}(\vec{r})$. When $\Delta\overleftrightarrow{\epsilon}(\vec{r})$ is periodic in x, with period d, the solution to the wave equation is

$$\vec{E}_j = \frac{1}{d}\int_0^d \overleftrightarrow{G}_j(x', z') \Delta\overleftrightarrow{\epsilon}(x', z') \vec{E}^{(0)}(x', z') dx' dz'\,, \tag{SI18}$$

where the dyadic Green function is given by

$$\overleftrightarrow{G}_j(x', z') = \frac{ik^2}{2k_{j,z}} \exp\left(-i\,k_{j,x}x' - ik_{j,z}z'\right) \left(\hat{s}_j\hat{s}_j + \hat{p}_j\hat{p}_j\right), \tag{SI19}$$

and the outgoing polarization basis vectors are

$$\hat{p}_j = -(k_{j,z}/k)\hat{x} + (k_{j,x}/k)\hat{z}, \tag{SI20}$$

$$\hat{s}_j = \hat{y}. \tag{SI21}$$

Thus, the outgoing wave in the jth diffraction order is

$$\vec{E}_j = -\frac{ik^2}{2dk_z}\exp\left(-\frac{\alpha\tau}{2\cos\theta_0}\right)\int_0^d (\hat{s}\hat{s}+\hat{p}\hat{p})\cdot\Delta\overleftrightarrow{\epsilon}(x',z')\cdot\vec{E}_{\text{in}}\,\mathrm{e}^{-i(k_x-k_{0,x})x-i(k_z-k_{0,z})z}dx'dz'\,. \quad \text{(SI22)}$$

Note that $\hat{s}\hat{s}+\hat{p}\hat{p}$ is simply the projection operator onto the plane perpendicular to the direction of outgoing propagation. If the measurement is polarization sensitive and measures a state along a unit vector $\hat{E}_{\text{out}}$ [and note that $\hat{E}_{\text{out}}\cdot(\hat{s}\hat{s}+\hat{p}\hat{p})=\hat{E}_{\text{out}}$], the efficiency for the j-th diffraction order is given by

$$\frac{P_j}{P^{(0)}} = \frac{k^2}{4d^2\cos\theta\cos\theta_0}\exp\left(-\frac{\mu\tau}{\cos\theta_0}\right)S \quad \text{(SI23)}$$

where

$$S = \left|\int_0^d \hat{E}_{\text{out}}\cdot\Delta\overleftrightarrow{\epsilon}(x',z')\cdot\hat{E}_{\text{in}}e^{-i(k_{j,x}-k_{0,x})x-i(k_{j,z}-k_{0,z})z}dx'dz'\right|^2 \quad \text{(SI24)}$$

and $\hat{E}_{\text{in}}$ is a unit vector in the direction of $\vec{E}_{\text{in}}$.

Comparison of Born approximation and RCW

The following two figures compare the Born approximation and RCW simulations at the P and S polarizations for the same optical constants as Figure 2 of the main text, but with θ_{in} as the x-axis instead of q_z. It can be seen that the two simulations match closely at both polarizations, deviating more at intensity minima.

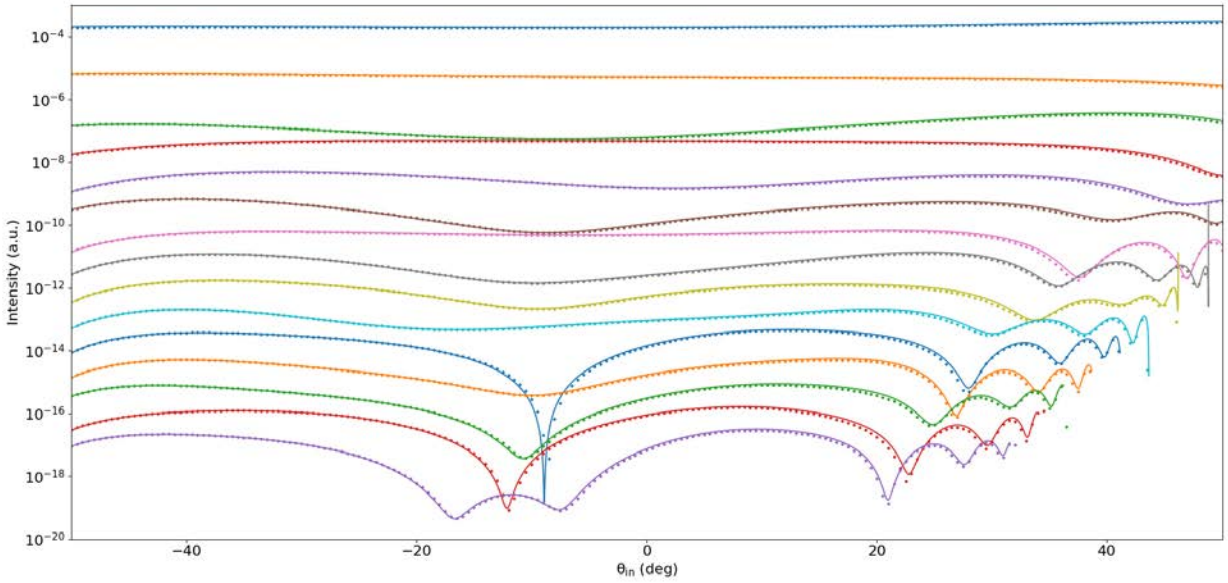

Figure SI1: Comparison of the Born approximation and RCW CDSAXS simulations for a stack of 3 trapezoids, P polarization. Each line (vertically offset for display) is for a different diffraction order from 1-15 and $-50° \leq \theta_{in} \leq 50°$. Lines are from Born approximation and points are from RCW.

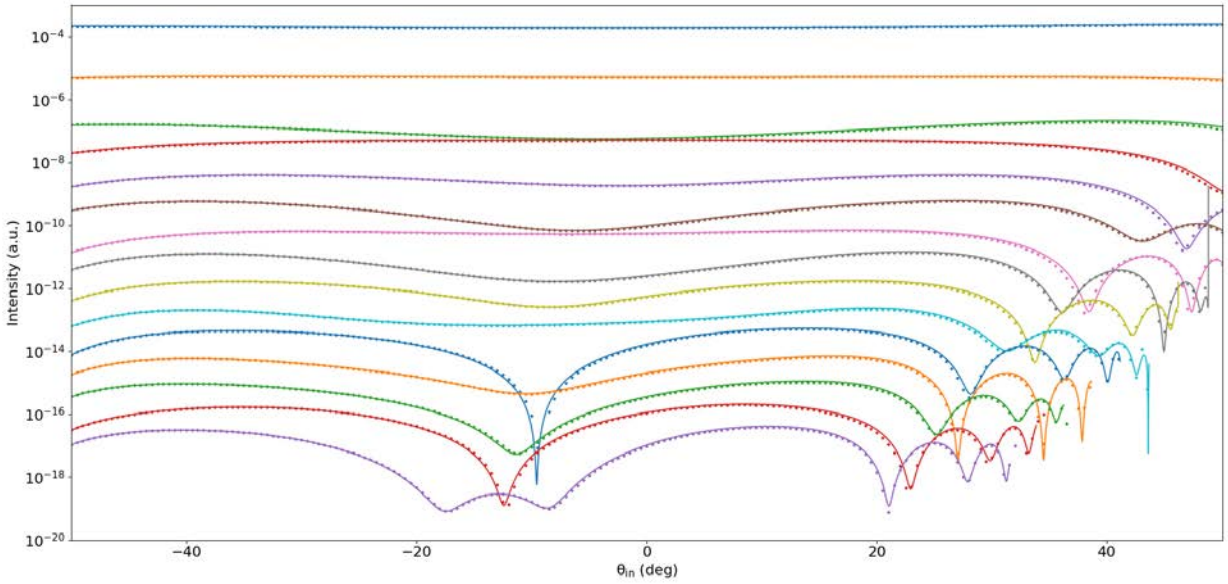

Figure SI2: Comparison of the Born approximation and RCW CDSAXS simulations for a stack of 3 trapezoids, S polarization. Each line (vertically offset for display) is for a different diffraction order from 1-15 and $-50° \leq \theta_{in} \leq 50°$. Lines are from Born approximation and points are from RCW.

Fitting simulated data for different sample models

The following target optical parameters were used for the sample models discussed in the main text:

Name	f_{x1}	f_{y1}	f_{x2}	f_{y2}	f_{x3}	f_{y3}	l_p (Å)
A	0.1	0.1	-	-	-	-	-
B	0.8	0.1	0.5	0.1	0.1	0.1	-
C*	0.1	0.1	-	-	-	-	20
D*	0.1	0.1	-	-	-	-	20
E	0.1	0.1	-	-	-	-	-
F	0.1	0.1	-	-	-	-	-
G	0.1	0.1	-	-	-	-	-
H	0.8	0.1	0.5	0.1	0.1	0.1	-
I*	0.1	0.1	-	-	-	-	20

*Table SI1: Target orientation factors and persistence lengths for each sample model. Trapezoid 1 refers to the bottom trapezoid, 2 to the middle, and 3 to the top trapezoid. "-" Refers to all trapezoids being constrained to have the same orientation factors. *Refers to interface orientation factors.*

The following table lists the goodness of fit for the various sample models. Ω_{target} represents how well the target parameters fit the target scattering with Poisson noise, and Ω_{fit} represents how well the best fit parameters of each run fit the target scattering with Poisson noise. Ω_{target} and Ω_{fit} are similar to each other for most of the sample models, except for models D and I (orientation), where the target and fit models are different and therefore Ω_{fit} is significantly worse than Ω_{target}. For models E-G where the target and fit models are different, fitting additional data in model F increases Ω_{fit} slightly but increases

the standard deviation of Ω_{fit} by a large amount. Both Ω_{target} and Ω_{fit} become worse with increased amounts of Poisson noise in model B.

Name	Ω_{target}	$min(\Omega_{target})$	Ω_{fit}	$min(\Omega_{fit})$
A	0.0323 ± 0.0019	0.0287	0.0320 ± 0.0021	0.0285
B (0.01)	0.0089 ± 0.0003	0.0080	0.0087 ± 0.0003	0.0079
B (0.1)	0.0285 ± 0.0010	0.0260	0.0280 ± 0.0010	0.0255
B (1)	0.0964 ± 0.0045	0.0893	0.0957 ± 0.0043	0.0881
C	0.0304 ± 0.0010	0.0283	0.0298 ± 0.0010	0.0277
D	0.0307 ± 0.0011	0.0282	0.0405 ± 0.0015	0.0370
E	0.0298 ± 0.0012	0.0272	0.0311 ± 0.0013	0.0285
F	0.0248 ± 0.0006	0.0238	0.0357 ± 0.0108	0.0289
G	0.0298 ± 0.0006	0.0287	0.0314 ± 0.0006	0.0300
H, I (morphology)	0.0207 ± 0.0010	0.0183	0.0204 ± 0.0010	0.0182
H (orientation)	0.0300 ± 0.0008	0.0284	0.0299 ± 0.0008	0.0282
I (orientation)	0.0308 ± 0.0009	0.0286	0.0505 ± 0.0011	0.0477

Table SI2: Goodness of fit statistics for 60 CMAES fitting runs (mean ± 1 standard deviation). Notable values are in red.

The following figure shows the correlation coefficients for the models shown in Figure 4 of the main text. For models A and C in which all trapezoids have the same orientation in the bulk, the shape parameters are highly correlated, especially the heights of adjacent trapezoids which are negatively correlated. For model B, in which all trapezoids have different orientation, the shape parameters are much less correlated, while the orientation parameters are correlated due to the constraint between them. Finally, for model D with different target and fit models, correlations are weaker overall due to the large variance in best fit parameters between runs.

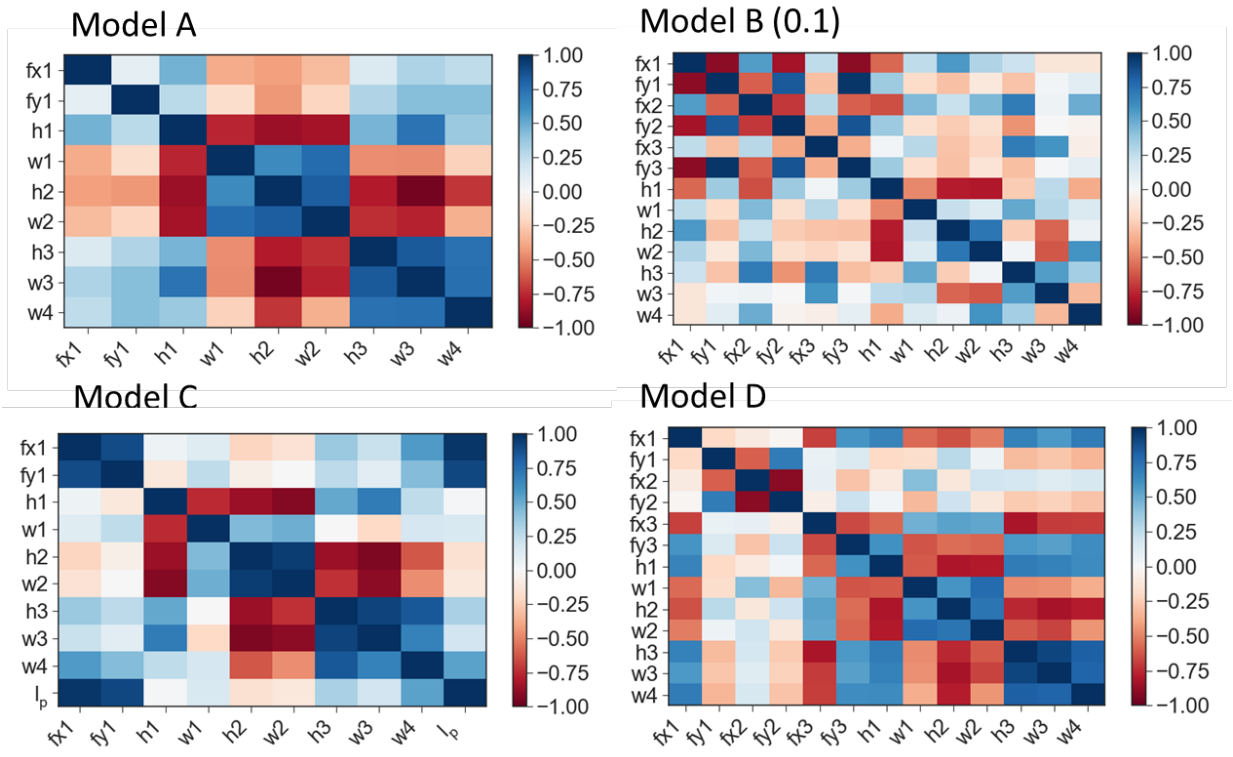

Figure SI3: Spearman's correlation coefficient for best fit parameters of each run from 60 independent CMAES fitting runs each of models A-D.

The following figure shows the correlation coefficients for all the models in the main text calculated from the MCMC chains instead of the CMAES runs, thus representing the local fitness landscape instead of the global fitness landscape. As stated in the main text, the parameters are much less correlated in the local fitness landscape than in the global fitness landscape. This suggests that the fitness landscape contains multiple correlated minimum valleys surrounded by slopes where the parameters are not as correlated.

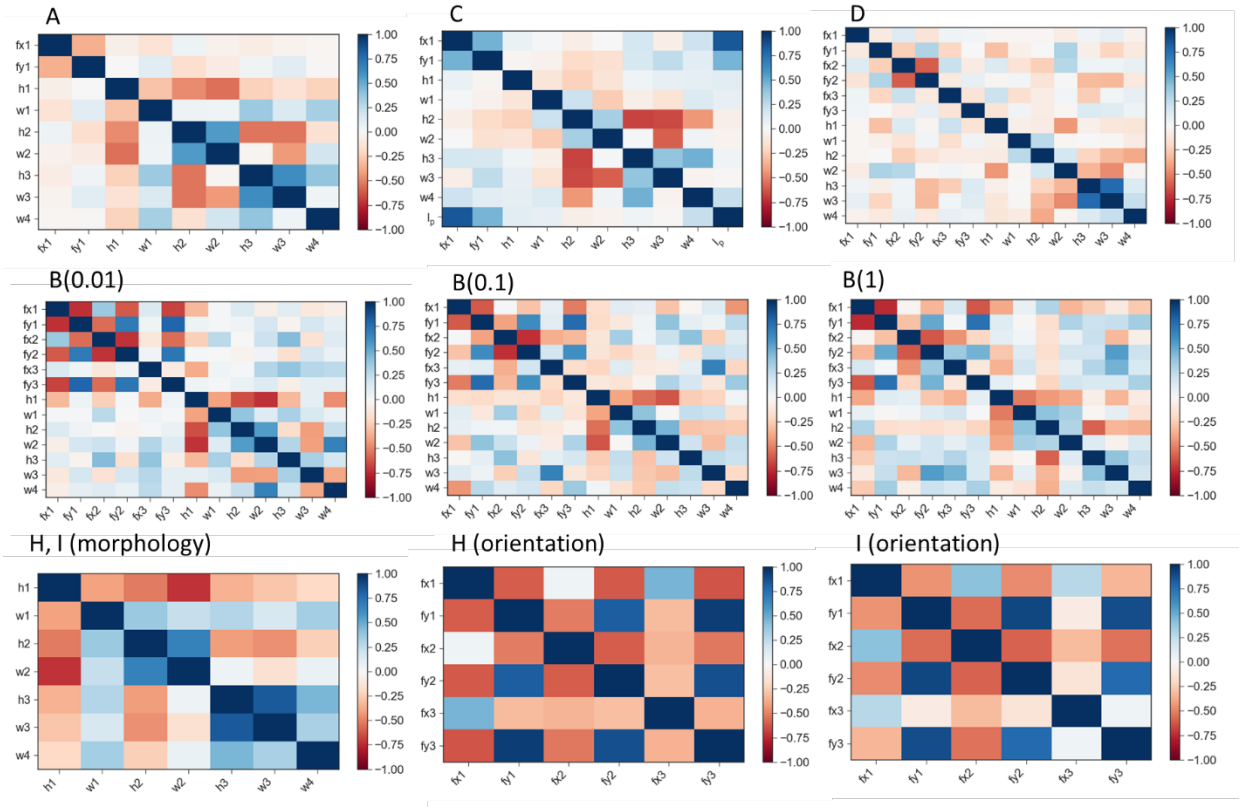

Figure SI4: Spearman's correlation coefficient for several target models, each with 30 MCMC chains starting at the best CMAES fit with a length of 100000 steps, resampled every 25 steps.

Several additional samples were run which are not mentioned in the main text:

Name	Asymmetric	Target model	Fit model	Poisson seed	Energies (eV)	Polarizations
SI1	No	Optical constants	Same as target	Same	284.2	P
SI2	No	Orientation factors	Same as target	Same	284.2	P
SI3	Yes	Orientation factors	Same as target	Same	284.2	P
SI4	Yes	Orientation factors	Same as target	Different	270, 284.2	P, S
SI5	Yes	Orientation factors	Same as target	Different	284.2 (x4)	P (x4)

Table SI3: List of additional sample models. Each sample model is composed of a target sample model, which is run once with the target parameters to generate the target scattering, and a fit sample model, which is run many times with iterated parameters to fit the target scattering.

For models SI1-SI3 the random seed of the Poisson noise is the same for each fitting run. This simulates the effect of fitting the same data multiple times and shows the variation as a result of the fitting algorithm as opposed to experimental noise. Model SI1 directly varies β and δ instead of the orientation factors as in model SI2. This tends to result in larger variations in the best fit parameters and less unique fits. The optical parameters in model SI1 are also much more correlated than in models using orientation factors, such as SI2. I_0 was not varied for model SI1 because it is effectively the same as multiplying all the optical constants by a constant. Model SI2 is similar to model A and model SI3 is similar to model B, but with the same seed for each fitting run. The errors between the best fit and target parameters are centered about a non-zero value depending on the seed, and have much less variance than when the random seed of the Poisson noise is different for each fitting run.

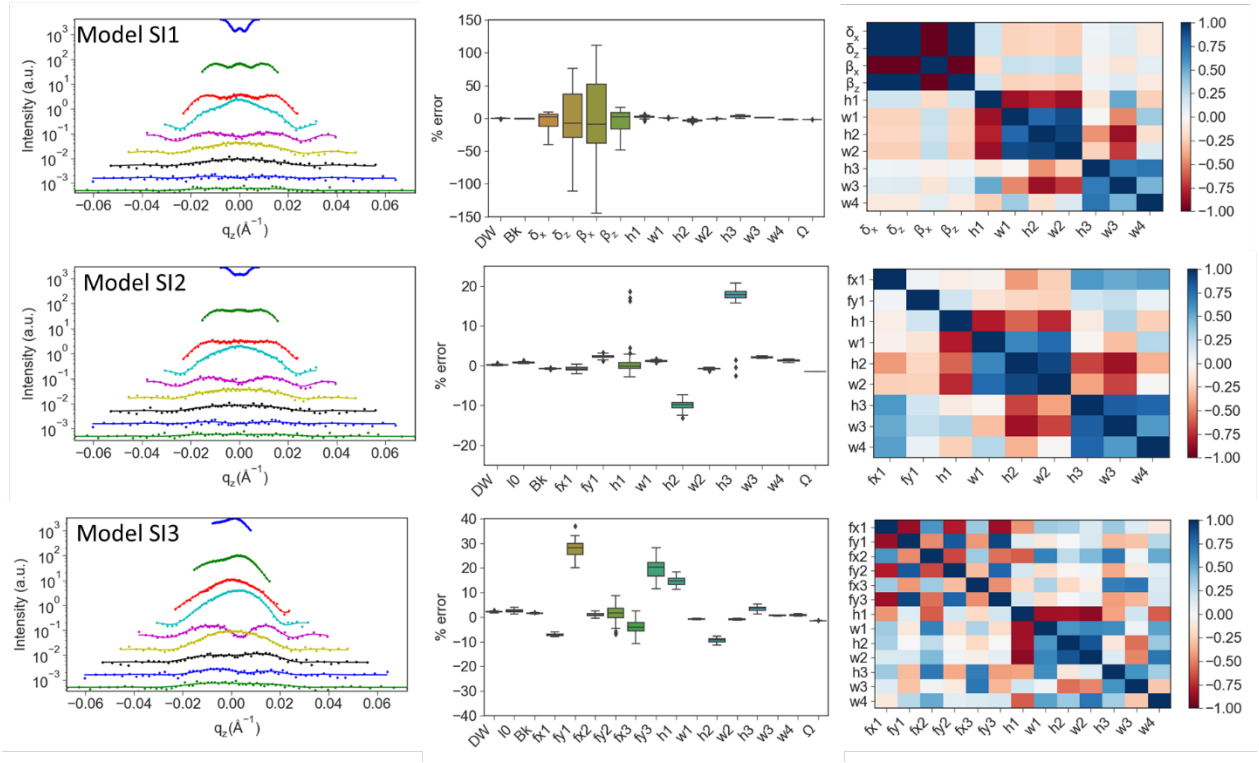

Figure SI5: Results from 60 independent CMAES fitting runs each of models SI1-SI3 where the random seed for the Poisson noise is the same for each fitting run. From left to right: the target scattering (vertically offset for display) with Poisson noise (dots) and best fit (lines), boxplots for percent error between best fit parameters and target parameters of each run, and Spearman's correlation coefficient for best fit parameters of each run.

Models B, SI4, and SI5 are similar to models E, F, and G respectively in the main text, except that the target and fit models are the same in the former set and different in the latter set. The variation in best fit parameters significantly decreases when going from model B to both SI4 and SI5, as more data is simultaneously fitted. SI4 and SI5 have about the same variation in best fit parameters even though SI4 has more information due to fitting two energies and two polarizations, while SI5 has four repeated simulated measurements with different Poisson noise. This contrasts with models F and G where there is a large difference between repeated simulated measurements and measurements with more unique information.

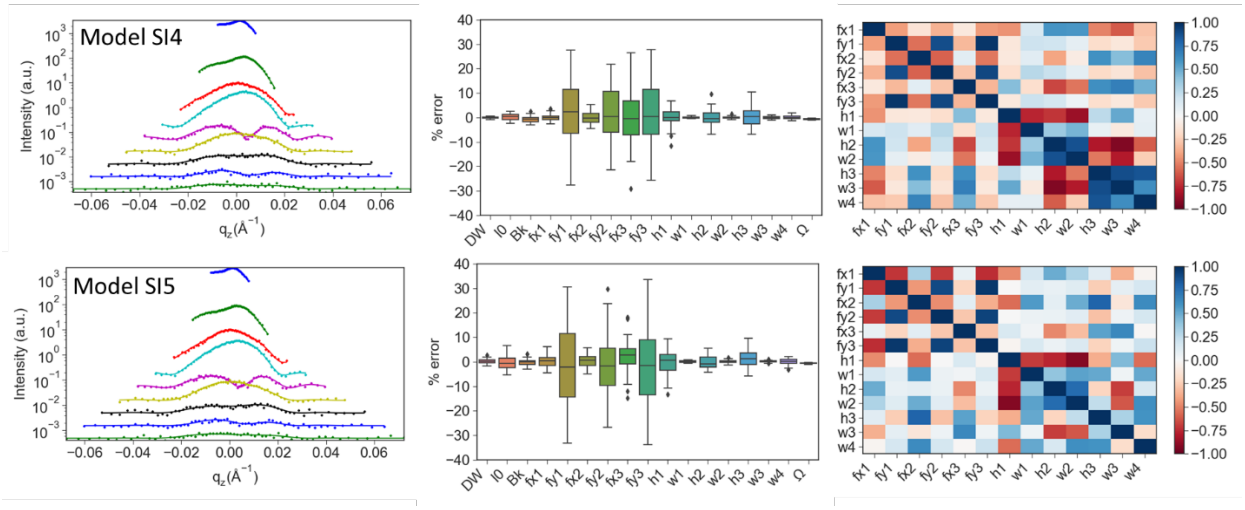

Figure SI6: Results from 60 independent CMAES fitting runs each of models SI4-SI5 with either different energies/polarizations or duplicate energies/polarization datasets with different noise. From left to right: the target scattering (vertically offset for display) with Poisson noise (dots) and best fit (lines), boxplots for percent error between best fit parameters and target parameters of each run, and Spearman's correlation coefficient for best fit parameters of each run.

References

Jackson, J. D. (1999). Classical Electrodynamics Wiley, 3rd edn.